In situ infrared by H. Seki spectroscopy of the electrode— electrolyte interface

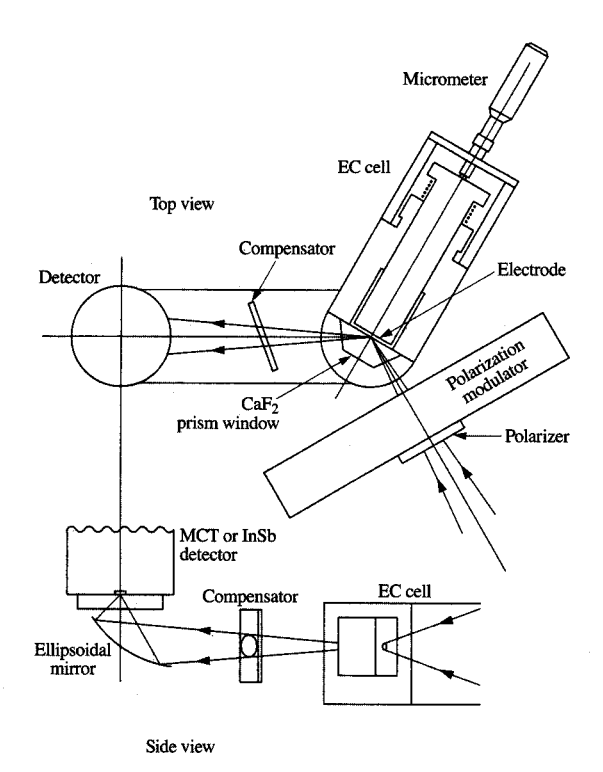
In the study of electrochemical processes, it is important to have a means for characterizing the molecular and ionic species at the electrode-electrolyte interface. Various types of optical vibrational spectroscopy are being used to do this in situ. Of these, Fourier transform infrared reflection absorption spectroscopy (IRRAS) has seen rapid progress and is in wide use. A review of the techniques used in our laboratory and examples of recent measurements are presented. The adsorbed species discussed are CO, CN⁻, SO₄²⁻, and HSO,, and the electrodes are, in most cases, polycrystalline noble metals. It is shown how the interpretation of the infrared spectra is greatly aided by comparison with ab initio molecular orbital computations of ions and molecules on metal clusters. Some of the difficulties in the interpretation of the infrared spectra are illustrated, and the future development of optical vibrational spectroscopy for studying electrodeelectrolyte interfaces is discussed.

Introduction

The first step in an electrochemical process takes place at the electrode-electrolyte interface. An important goal of modern electrochemistry is to gain an understanding of this interface at the molecular level. The discovery of surfaceenhanced Raman scattering (SERS) [1, 2] and the demonstration of straightforward, modulated specular reflectance spectroscopy in the infrared region [3] in the early 1980s have combined to provide a means to investigate in situ the electrode-electrolyte interface with a relatively high degree of molecular specificity. Although the extremely high sensitivity of SERS attracted considerable attention initially, the underlying mechanisms turned out to be more complex than had initially been expected [4]. Furthermore, the electrode surface generally requires some pretreatment, which gives it an ill-defined atomic scale roughness, and the enhancement is limited to metals such as Ag, Au, and Cu. On the other hand, the rapid development of reliable Fourier transform infrared (FTIR) spectrometers and sensitive infrared detectors has made infrared spectroscopy the more general technique for investigating the electrode-electrolyte interface.

In this paper some of the work involving in situ FTIR spectroscopy, carried out primarily in our laboratory, is reviewed, illustrating the associated insights we have been able to obtain. Since infrared reflection absorption spectroscopy (IRAAS; sometimes designated as IRAS) on well-defined single-crystal electrodes is a very important development to which we have not yet contributed, we also include some of the significant results in that area that have come to our attention. Thus far, most of the spectra

Copyright 1993 by International Business Machines Corporation. Copying in printed form for private use is permitted without payment of royalty provided that (1) each reproduction is done without alteration and (2) the Journal reference and IBM copyright notice are included on the first page. The title and abstract, but no other portions, of this paper may be copied or distributed royalty free without further permission by computer-based and other information-service systems. Permission to republish any other portion of this paper must be obtained from the Editor.



Schematic diagram of the optical configuration and electrochemical cell for obtaining PM-FTIRRAS. From [8], reproduced with permission.

are taken in the double-layer potential region, where the Faradaic current is negligible and the electrode surface condition is reversible with respect to its potential. In this respect we are still in the very early stages of understanding electrochemical processes. It will be seen that for relatively simple adsorbates considerable insight is gained when the results obtained by vibrational spectroscopy are considered in conjunction with the results of *ab initio* self-consistent field (SCF) cluster-adsorbate calculations.

Experimental procedures

IRRAS was first used in connection with the gas-metal interface, and was pioneered by Greenler [5]; the details of the underlying theory can be found in a number of earlier papers [6]. Because of the boundary condition that the electric field along a highly conducting surface must be zero, the formula derived for light reflection shows that at the metal surface the E-vector of light polarized perpendicular to the plane of incidence (s-polarized) goes

to zero, while the E-vector is enhanced by almost a factor of 2 for light incident at grazing angle and polarized parallel to the plane of incidence (p-polarized). The result is the so-called "surface selection rule"; i.e., at a grazing angle of incidence, a molecule on the metal surface absorbs only p-polarized light if it has a component of its dynamic dipole moment perpendicular to the surface.

This principle is also applied to the electrode–electrolyte surface, but in this case there is the additional problem of infrared light absorption by the solvent, which is particularly strong for water. The absorption of light is minimized by a thin-layer design of the electrochemical cell [3]. The cell used in our laboratory is shown in **Figure 1** and has been fully described elsewhere [7]. Its body is made of chemically inert Kel-F, and the electrode is mounted on a piston so that its surface can be spaced at a distance of about 1–3 μ m from the optical window, in order to minimize the signal from the bulk electrolyte.

Various techniques have been developed to minimize the background and highlight the infrared spectra of the species on the electrode, and with them a number of acronyms have evolved. These include EMIRS (electrochemically modulated infrared spectroscopy) [9], SNIFTIRS (subtractively normalized interfacial Fourier transform infrared spectroscopy) [10], PDIRS (potential difference infrared spectroscopy) [11], and SPAIRS (single potential-alteration IR spectroscopy) [12]. Each technique involves taking the spectral difference between two potentials in order to reduce the contributions that arise along the optical path due mainly to the solvent, window, and gases, and to improve the signal-to-noise ratio; a discussion of the details involved has been given by Corrigan et al. [12]. In our laboratory we use the IBM Instruments IR/98 FTIR (Fourier transform infrared) spectrometer and, in addition to PDIRS, we often employ PM-FTIRRAS (polarization-modulated FTIR reflection absorption spectroscopy). This latter technique has evolved from the work of Golden et al. [13, 14] and uses a photoelastic modulator to switch the polarized infrared beam (incident at ~60°) between p and s polarization. It takes advantage of the surface selection rule mentioned earlier to obtain essentially the infrared absorption spectra of the species very close to the electrode surface which have dynamic dipole moments with components normal to the surface. The detector signal consists of an ac component corresponding to $(I_p - I_s)$ and a dc component corresponding to $(I_p + I_s)$, where I_p and I_s are the detected intensities of the p- and s-polarized light. By circuitry outlined elsewhere [14], we obtain $(I_p - I_s)/(I_p + I_s)$.

Of all the techniques listed above, the main advantage of the PM-FTIRRAS technique is that $(I_p - I_s)$, which

¹ We have been using the Hinds International PEM-80 Series II ZnSe photoelastic modulator, which modulates the polarization at 74 kHz.

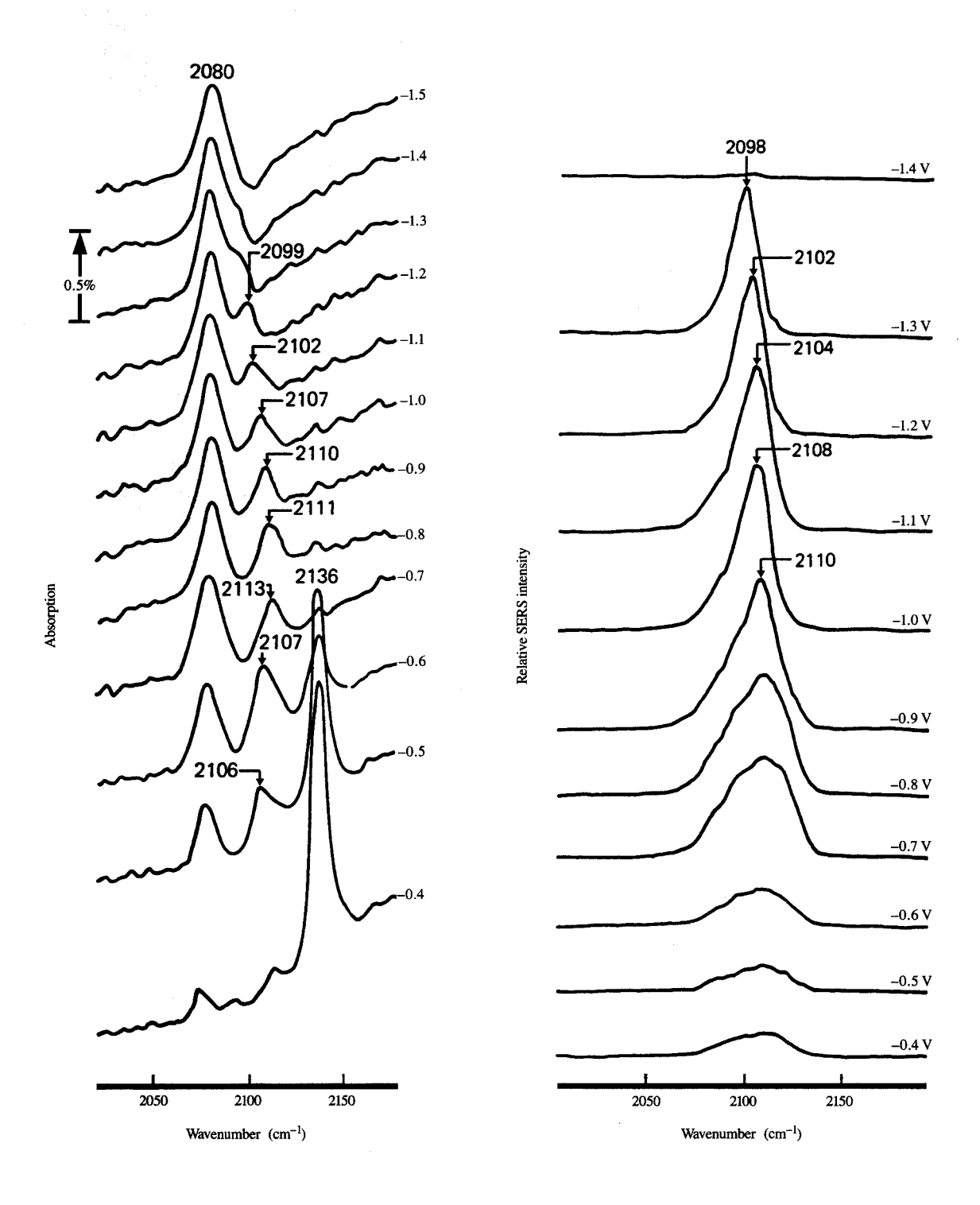
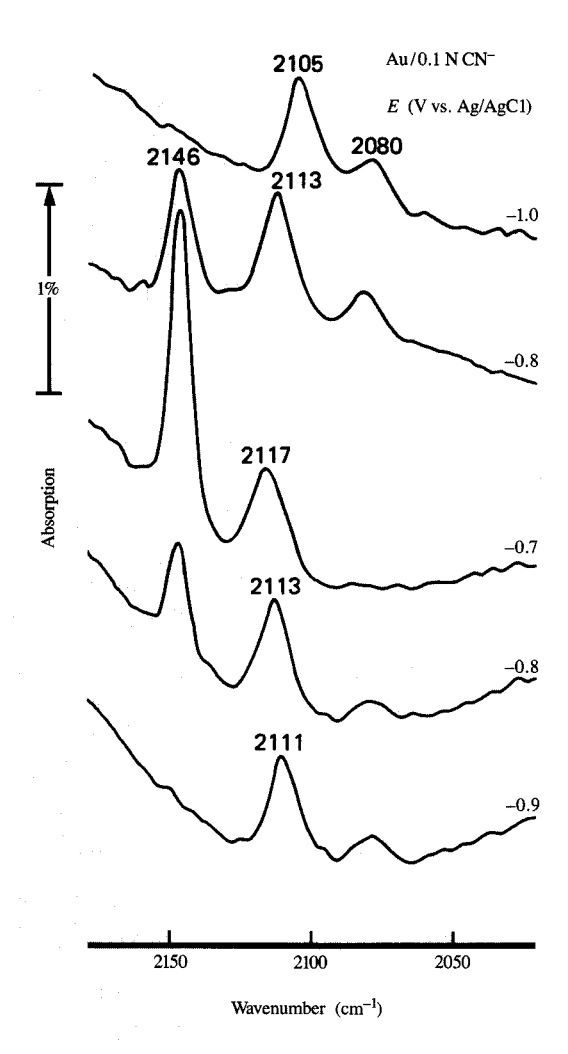


Figure 2

Typical PM-IRRAS (left) and SERS (right) spectra for an Ag electrode in an aqueous 0.01~M cyanide solution at potentials of -0.4~V to -1.4~V (Ag/AgCl). From [21], reproduced with permission.



Reversible change of the PM-IRRAS spectra associated with the Au/0.01 M CN interface when the potential is changed from -1.0 V to -0.7 V and reversed. From [25], reproduced with permission.

contains the absorption spectra of the species on or near the electrode surface, is amplified directly by the lock-in amplifier before digitization. The dynamic range limitation of the analog-to-digital converter in the FTIR is in effect bypassed by this process [15], resulting in a high signal-to-noise ratio. Furthermore, this is done at a fixed potential, and the band shape is observed directly. These are important factors when the objective is to obtain weak submonolayer signals.

The optical configuration which we have used recently for IRRAS is shown in Figure 1. This arrangement has fewer beam reflections after the sample compared to what was shown in an earlier paper [7]. The highest sensitivity is obtained by using an InSb detector, but this places a lower limit on wavenumber of about 1850 cm⁻¹. With a slight sacrifice in sensitivity, use of a HgCdTe (MCT) detector and a ZnSe cell window extends the limit in the low-energy region down to about 700 cm⁻¹.

Adsorption of cyanide

The cyanide ion is a relatively simple diatomic ion, but it is of fundamental interest in electrochemistry. Nevertheless, our knowledge of how it is adsorbed on a metal surface is rather precarious. This can be seen in the various adsorption models which have been proposed in relation to the spectra obtained through SERS. These have ranged from simple linear bonding through carbon to ionic complexes such as $[M(CN)_n]^{(n-1)^-}$, where M is Ag or Au and n is 2 or 3 [16–20]. Infrared investigation of the electrode in cyanide solution has helped clarify the structure of the adsorbate for the Ag and Au electrodes.

A comparison of SERS and PM-FTIRRAS is also useful in order to illustrate the features of the spectra that are obtained. Figure 2 contains examples of spectra taken by PM-FTIRRAS and SERS for evanide in aqueous media on Ag [21]. A striking characteristic about the SERS spectra is that only one band is present, which can be attributed to the surface-adsorbed cyanide because of the very short range of SERS. In contrast to this, the series of infrared spectra on the left displays three distinct bands [22, 23]. This is because the spectra taken with p-polarized light detect not only the adsorbed ions but also species in the vicinity of the electrode. This is the main difference between the electrochemical IRRAS and the IRRAS of the metal-gas interface, in which the absorption due to the gas-phase species is absent because their concentration is too low for detection. The bands at 2080 cm⁻¹ and 2136 cm⁻¹, which do not change their band positions, are readily assigned to solution-phase cyanide ion and [Ag(CN)₂] complex, respectively, in agreement with reported values [24]. The third band, at about 2100 cm⁻¹, shifts to lower wavenumbers as the electrode potential becomes more negative and matches the main band in the SERS spectra. This potential-dependent shift of the absorption band is an indication that the band can be assigned to a surface species; this is often used in the interpretation of IRRAS data. If the surface species were a dicyano complex, it could be bent with a C_{2v} symmetry and would display vibrational modes corresponding to the symmetric, Raman-active mode and the asymmetric, infrared-active mode, with frequencies that differ from each other. The near-perfect match of the IRRAS and SERS bands is consistent with the adsorbed species being a single "on-top" cyanide ion which is both Raman- and infrared-active. Similar results are obtained for cyanide on Au [23, 25]; i.e., the position and the potential-dependent

230

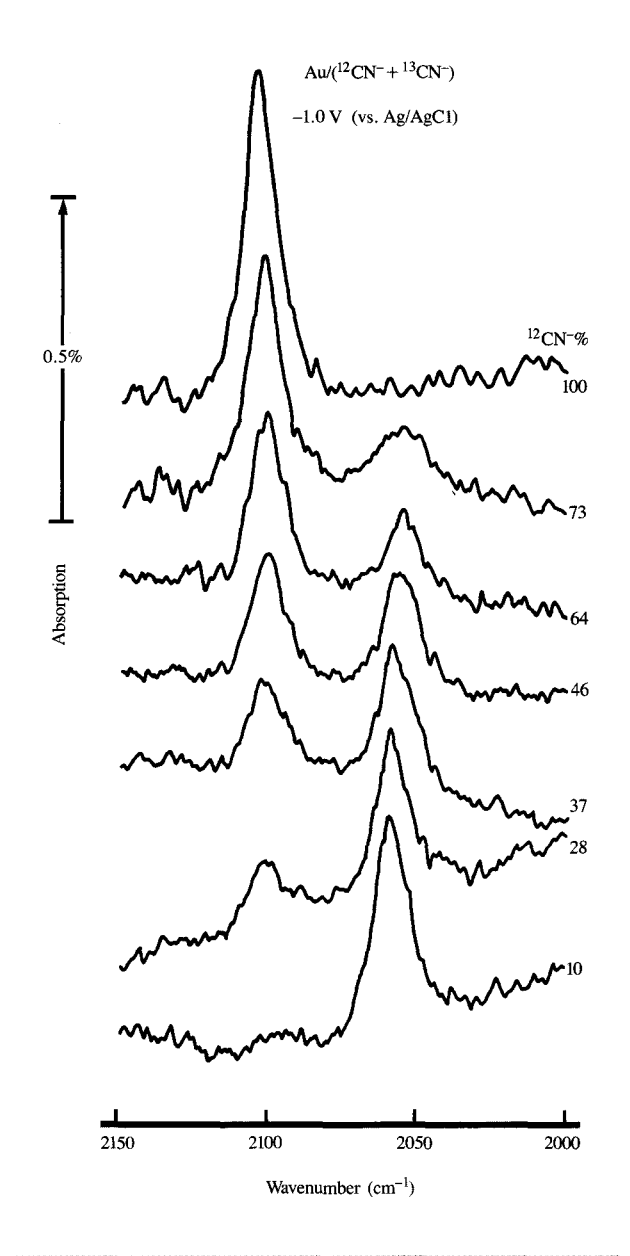
shift of the IRRAS and SERS bands of the adsorbed cyanide are identical.

Although the presence of absorption bands of nonsurface species adds complexity to the spectra, with proper interpretation it can also aid our understanding. This is seen in the reversible series of IRRAS spectra in Figure 3 for an Au electrode in a cyanide solution [25]. As the potential is stepped from -1.0 V to -0.7 V and then reversed, the 2146-cm⁻¹ band, which is assigned to the [Au(CN)₂] complex ion in solution [23, 25], undergoes a reversible increase and then a decrease. The appearance of the 2146-cm⁻¹ band is accompanied by the disappearance of the 2080-cm⁻¹ solution evanide band, and vice versa. When the potential drops to -0.9 V, all of the $[\text{Au}(\text{CN})_3]^$ complex in solution is reduced, as indicated by the disappearance of the 2146-cm⁻¹ band. It is highly improbable that the complex could remain unreduced on the gold surface at potentials more negative than -0.9 V. The frequency-shifting band around 2100 cm⁻¹ must therefore be assigned to a single cyanide, linearly bonded to the surface through the carbon atom.

Since the band of the surface cyanide is slightly sharper for IRRAS than for SERS, isotope experiments were carried out with IRRAS, partly to reexamine the SERS isotope experiments reported by Fleischmann et al. [18]. In **Figure 4** a series of spectra are shown, each for a different ratio of ¹²CN⁻ and ¹³CN⁻. The total concentration of the cyanide was maintained at 0.01 M and the spectra were taken at -1.0 V, a potential at which the single-isotope ¹²CN⁻ solution gave the maximum intensity.

Although a slight shift in the band frequency is seen with the change in composition (which is discussed later), there is no noticeable line broadening, which would have been expected due to the formation of some mixed isotope complexes, if the surface species were a dicyano complex. The fact that there are only two distinct frequency bands in the presence of the two isotopes regardless of their ratio supports the single cyanide surface model. This conclusion is also consistent with the cluster-adsorbate computations which are discussed later. At this point, it is sufficient to say that calculations performed for the single linearly adsorbed cyanide could account for all of the essential spectral observations.

An important parameter available in electrochemical systems is the electrode potential. By controlling the electrode potential, very high electric fields, up to the order of 10⁷ V/cm, can be applied to an adsorbed molecule or ion; this is not easily accomplished for metal-vacuum or metal-gas interfaces. The first observation of a field-dependent shift of the vibrational band was reported in 1981 by SERS investigators [26, 27], i.e., the shift with potential of the SERS band from an Ag electrode in cyanide solution. In the following year, potential-dependent shifting in the CO stretching band was observed



Change in the IR bands of the adsorbed CN^- with isotopic composition of $^{12}CN^-$ and $^{13}CN^-$ while the electrode potential was at -1.0~V and the total cyanide concentration in the solution was 0.01~M/l. From [25], reproduced with permission.

with IRRAS [28, 29]. Experiments have also been carried out for CO on Ni in UHV (ultrahigh vacuum) [30], but for lower applied fields. Since the detection of infrared spectra is not dependent on special active sites, as in SERS, and the bands are slightly narrower, the use of PM-IRRAS is especially suitable for studying the potential-dependent

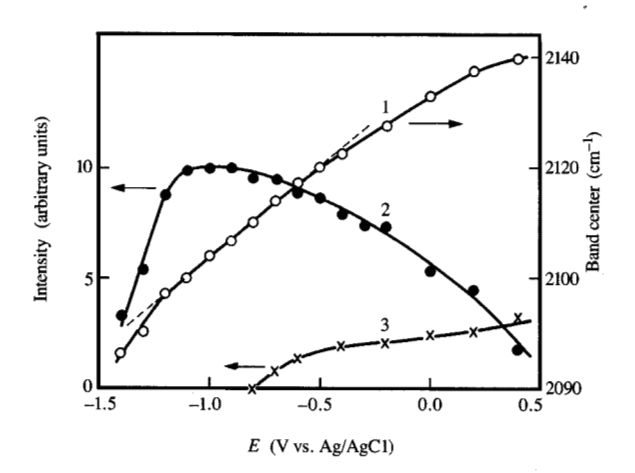
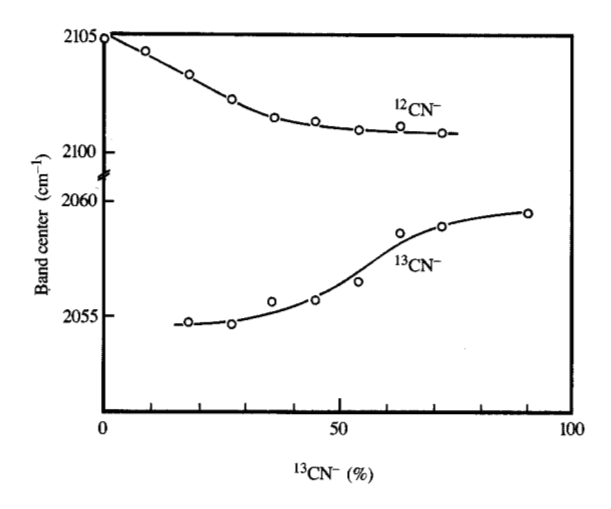


Figure :

Potential dependence of (1) the IR band center, (2) the integrated band intensity of adsorbed CN^- on Au, and (3) the integrated band intensity of the $[Au(CN)_2]^-$ complex. From [25], reproduced with permission.



Faure 6

Dependence of the position of C-N stretching frequency of the adsorbed ¹²CN and ¹³CN on the isotopic composition based on the data of Figure 4. From [25], reproduced with permission.

behavior. Studies have been made of CO on Pt [31, 32] and CN on Ag [22, 23], Au [23, 25], Cu [33], Pt [34], and Pd [34, 35] using this technique.

The potential-dependent frequency shift of the CN band for an Ag electrode can be seen in Figure 2. In Figure 5 the band position as well as the integrated band intensity is plotted as a function of the potential for an Au electrode [25] in a cyanide solution. It is interesting that both the direction of the potential shift and the shift of ~30 cm⁻¹/V for the cyanide band on Ag and Au [22, 23, 25] are essentially the same as for the CO band on Pt [31]. It was found that the intensity of the CO band, i.e., the surface concentration of CO, is constant over most of the potential range in which the band was observed, indicating that the observed potential shift is mainly field-dependent. This was also seen with the cyanide band, as indicated in Figure 5; the frequency position shift is approximately linear between -1.2 and -0.5 V (Ag/AgCl), where the integrated band intensity changes slowly. However, as the band intensity decreases with increasing potential, the shift of the band position with potential also decreases; this is attributed to lower lateral interaction of the adsorbates due to decreased surface concentration. This effect of surface concentration is more clearly seen in Figure 6, where the results of Figure 4, all taken at the same potential, are plotted explicitly as band position versus percentage of ¹³CN⁻. This effect of the surface concentration on the frequency is consistent with the coverage-dependent frequency shift observed for adsorbed CO in UHV [36-38]. We note that the net shift that can be induced by the electrode potential is about an order of magnitude greater than that resulting from concentration changes.

The most widely accepted model of a CO molecule linearly adsorbed on a metal, based on studies of metal carbonyls [39], is with its carbon atom adjacent to the metal. The bond is covalent with the lone pair 5σ orbital donating charge to the metal while there is a π backdonation into the empty CO $2\pi^*$ level [40]. The occupation of the antibonding $2\pi^*$ orbital weakens the C-O bond and causes the lowering of the C-O vibration of the adsorbed CO molecule. Thus, it is reasonable to conjecture that this balance of charge exchange in the orbitals is affected by the applied field, altering the C-O force constant [41, 42]. Faced with the similarity of the potential-dependent band shift and the fact that CO and CN are isoelectronic, it could be argued that the observed potential-dependent shift is due to similar mechanisms for both CO and CN. Indeed, this explanation was proposed for the initial observation of the CN frequency shifts [43].

Lambert, however, proposed an interesting alternative explanation, i.e., that the potential-dependent frequency shift could be explained by a first-order Stark effect without involving a change in the covalent bonding due to the field [44]. This was demonstrated by calculating the Stark tuning rates using first-order perturbation theory and experimentally measured vibrational frequencies and

molecular constants of a number of molecules (including CO) in the gas phase.

SCF cluster calculations

The development by Bagus et al. of ab initio SCF wavefunctions for clusters has provided a powerful basis for interpreting the experimental observations related to the localized bonding of adsorbed molecules [45-49]. In these calculations, the metal surface is represented by a metal cluster which ranges in size from a single metal atom to over 30 metal atoms, the larger cluster generally giving more realistic results at the cost of increased computational time. Substitution of a metal cluster for the real surface is an approximation and weakens the validity of the computational results for phenomena involving extended states. However, the advantage of the ab initio method, that it does not involve adjustable parameters, is still quite persuasive and distinguishes it from other molecular orbital methods which include parameters that are adjusted to fit experimental results.

Very briefly, what this means is the following: The electrons in the system (cluster) are described by molecular orbitals which generally consist of a sum of a finite set of basis functions (e.g., atomic orbitals), each basis function having a coefficient. The wavefunction of the system is a Slater determinant of these molecular orbitals. The SCF wavefunction, for a given fixed position of the atoms, is determined by carrying out variational SCF computations of the total energy of the system; i.e., the coefficients of the basis functions are varied in order to select a set of coefficients which minimizes the energy of the system. There are no empirical parameters which can be adjusted to match the results to experiment. The investigator chooses the model for the calculation, i.e., the basis set, its size, the level of sophistication of the computation (e.g., configuration interaction), the cluster size, the use of pseudopotentials to approximate the core electrons of some of the metal atoms, etc. The validity of the computation is determined by these choices. Physical insight and computational experience are needed to make the appropriate selection of the computational model, depending on the information being sought. This usually involves trade-offs with the computational power and time available. (A more complete discussion of the ab initio methods can be found, for example, in [50].)

The degree of confidence we can have in the computational result is ultimately determined by the ability of the model to produce results which agree with experiments. As an example, the equilibrium interatomic distance of a molecule is obtained by computing the SCF energy for various atomic separations and finding the location for the minimum energy. The models used in the work here have been successful with regard to the

calculation of adsorption bond distances [46] and the interpretation of photoemission spectra [45].

Most of the calculations have been done for Cu, since it has the least number of electrons of the metals of interest. The clusters represent the Cu(100) surface, and the positions of the metal atoms are fixed by bulk fcc geometry. The adsorption site metal atom is usually treated with all its electrons, while the rest are treated with one 4s electron and a pseudopotential for the core electrons. The heavier metals can be studied by using pseudopotentials for all of the metals in the cluster. The adsorbed molecule is treated with all its electrons, and the equilibrium positions are determined by minimizing the SCF energy. The positions of the adsorbate atoms are varied around the equilibrium position, and SCF energies at several points are fitted to a potential surface to obtain the interatomic force constants and the vibrational frequency.

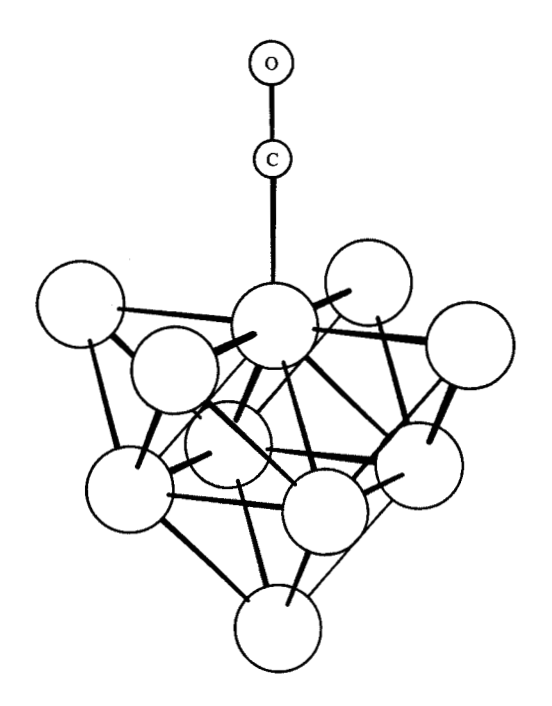
The *ab initio* SCF cluster wavefunction has been used to investigate the bonding of CO and CN $^-$ on Cu $_{10}(5,4,1)$ (five surface-layer atoms, four second-layer atoms, and one bottom-layer atom), and to calculate their field-dependent vibrational frequency shifts in fields up to 5.2×10^7 V/cm [48]. A schematic view of the Cu $_{10}(5,4,1)$ CO cluster is shown in **Figure** 7. In order to assess the significance of Lambert's proposal that the linear Stark effect is the dominant factor in the field-dependent frequency shift, the effect of the field was calculated by three methods. One involves the use of a fully variational approach (i.e., the adsorbate is allowed to relax under the influence of the applied field) in which the Hamiltonian for the cluster in a uniform electric field F is given by

$$H(F) = H(0) + F \sum_{i} r_{i} - F \sum_{i} R_{i},$$

where r_i and R_i are the position of the electrons and the nuclei of the adsorbate. The energy obtained from this Hamiltonian is $E_{\rm SCF}(F)$, and the resulting wavefunction includes the total effect of the field, changes in the chemical bonding, and the Stark effect. The second method involves the use of first-order perturbation theory energy, assuming that

$$E_{p}(F) = E_{SCF}(0) - \mu(0)F,$$

where $E_{\rm SCF}(0)$ and $\mu(0)$ are the zero-field SCF energy and dipole moment, respectively. The third method follows the formalism of Lambert [44], in which Taylor series expansions of the ligand potential and the dipole moment are used. The coefficients in the expansions are calculated from the zero-field SCF wavefunctions instead of using the measured molecular parameters, as was done by Lambert. The latter two methods can be used to calculate changes based on zero-field parameters and do not involve changes in the chemical bonding. (For a complete description and



Schematic view of the $Cu_{10}(5,4,1)CO$ cluster, simulating the Cu(100) surface with CO adsorbed at an "on-top" site. From [47(b)], reproduced with permission.

discussion of the SCF cluster analysis in general, [45–49] and references therein should be consulted.)

The frequency shifts calculated by the latter two methods agree quite well, as might be expected since both are essentially variations of first-order perturbation theory. More importantly, the differences between the shifts calculated by the fully SCF method and the perturbation methods are relatively small. This endorses the proposal by Lambert [44] that the frequency shifts due to fields less than the order of 10⁷ V/cm arise mainly from a first-order Stark effect. (A similar conclusion was claimed by Bauschlicher [51], but it was based only on results of SCF calculations on the isolated CO in an applied field parallel to the molecule.) The results of these analyses also showed that the metal-ligand bonding for CO and CN is quite different. In the case of CO, the bond is covalent with dominantly metal-to-CO $2\pi^*$ back-donation; for CN⁻, the bonding is mainly ionic. It is also interesting that the calculated bond energy did not change very much, when the orientation of CN was changed, consistent with the inference that covalency of the bonding is small. The fact

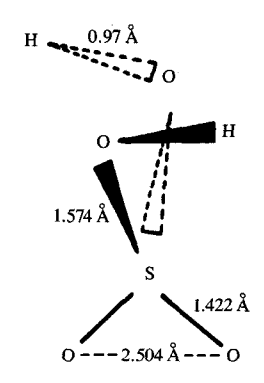
that the infrared intensity of the surface C-N stretch is weak on Cu is most likely an indication that all of the CN is not oriented perfectly normal to the surface. Since the intensity is stronger on Ag and Au electrodes, this may indicate that as the d shell of the metal is filled, the covalency of the metal ligand bond increases and the degree of normal orientation improves.

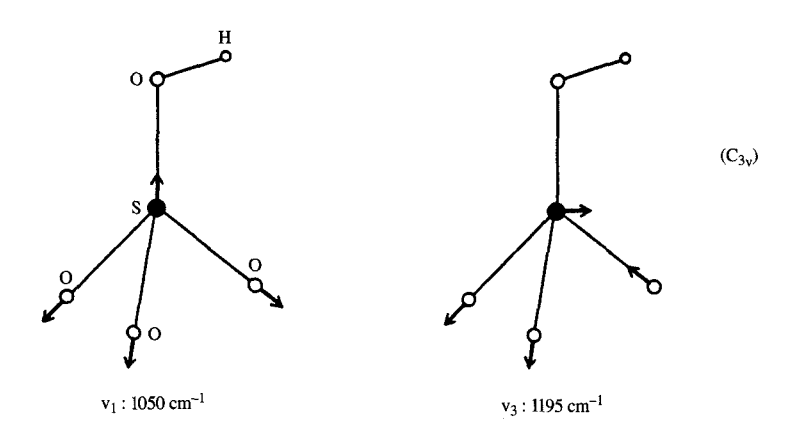
It is quite interesting that because of this difference in the bonding, the manner in which the field affects the frequency is different for the two adsorbates. In the case of CO, the change is a direct change in ligand frequency, but in the case of CN, the change in the calculated ligand frequency is considerably smaller than for CO. This does not agree with the experimental observation that the frequency shifts are comparable for CO and CN. This discrepancy has been resolved by recognizing that the ligand vibration and the metal ligand vibration are coupled. Because of the ionicity of the metal-CN bond, the Cu-C distance and the metal ligand frequency are changed appreciably by the applied field. Through the interaction between the two oscillators, the frequency of the normal mode corresponding to the C-N stretch is also increased. This has been investigated in more detail using a Cu₄(5,4,5)CO cluster [49] which can be visualized by surrounding the bottom Cu atom in Figure 7 with four more Cu atoms. In this study it was shown more clearly how the change in the Cu-C distance also causes a change in the ligand force constant because of a "wall" effect of the metal surface electrons; this brings the C-N vibrational frequency shift within a factor of 2 of the C-O frequency shift. The shift in the metal cyanide frequency was, in fact, reported in the initial SERS observation of the potentialdependent shifts [26, 27]. The final experimental verification of these analyses would be to determine whether the effect of the field on the metal-ligand stretching frequency in the far IR for CO is small, as our model predicts.

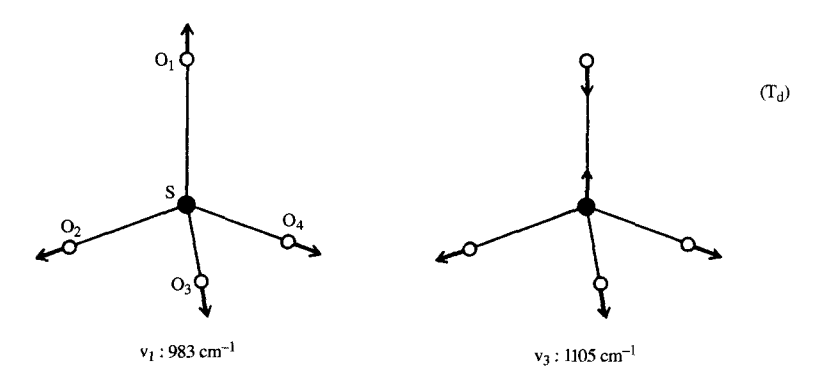
Bisulfate and sulfate adsorption on Pt

As a slightly more complex system, we have examined the platinum electrode in solutions of sulfuric acid [52–55]. Sulfuric acid in water dissociates in two steps into HSO₄ and SO₄²⁻ and, though it is known from radiotracer techniques that these anions adsorb on platinum electrodes as a function of electrode potential [56], the ratio of the two anions on the surface was not known until the IRAAS measurements. These measurements highlighted the unique capability of vibrational spectroscopy to distinguish similar but different molecular entities on a surface.

The structure and some of the dimensions of the sulfuric acid molecule are illustrated in **Figure 8**, together with some of the vibrational normal modes of the anions. The bisulfate ion, HSO_4^- , having C_{3v} symmetry, has a symmetric stretching mode at 1050 cm⁻¹ and an





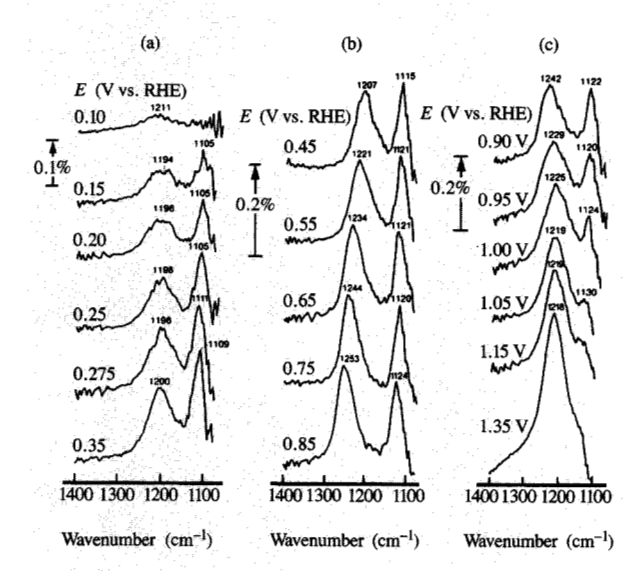


Emma.

Molecular structure of the H_2SO_4 molecule and two of the normal S-O stretching modes of the HSO_4^- and $SO_4^{2^-}$ anions. From [53], reproduced with permission.

asymmetric mode at 1195 cm $^{-1}$. Both Raman and infrared active modes are shown. For the sulfate ion, SO_4^{2-} , with T_d symmetry, the symmetric Raman active mode and the

asymmetric stretching mode at 1105 cm⁻¹, which is both Raman and infrared active, are shown. These are the bands observed by IRRAS. A typical series of associated

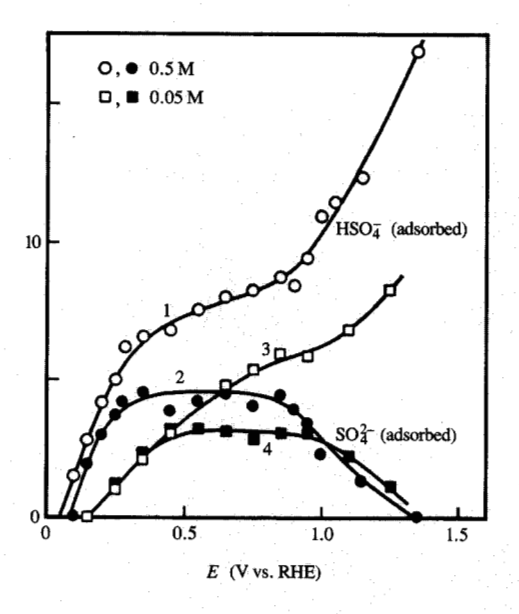


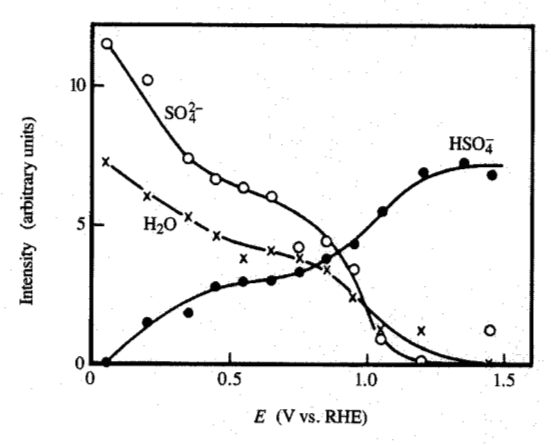


Potential dependence of the asymmetric S–O stretching bands of the ${\rm HSO}_4^-$ and ${\rm SO}_4^{2^-}$ anions around 1200 cm⁻¹ and 1100 cm⁻¹, respectively, adsorbed on Pt in 0.5 M ${\rm H}_2{\rm SO}_4$: (a) hydrogen region, (b) double-layer potential region, (c) oxygen region. From [53], reproduced with permission.

spectra obtained from a Pt electrode in $0.5~\mathrm{M}~\mathrm{HSO}_4^-$ is shown in Figure 9 [53]. The spectra were obtained using p-polarized infrared light in the PDIRS mode; each spectrum was normalized by the reference spectrum taken at $0.05~\mathrm{V}$ (RHE), where the radiotracer results showed negligible anion adsorption [56]. It is rather striking that although, on the basis of the dissociation constant of the bisulfate ion of $1.02~\mathrm{\times}~10^{-2}$, the sulfate/bisulfate concentration ratio of the solution was expected to be about $0.02~\mathrm{for}$ the solution, the surface concentration ratio of the anions based on the spectral band intensities was found to be considerably larger, assuming the same extinction coefficient for the surface species as for the bulk.

The spectra obtained via PDIRS were taken for solutions of varying pH values [52–55]. The results obtained are summarized in Figure 10, where the potential dependence of the S-O stretching band intensities of the adsorbed anions in the various solutions can be compared. Although at the time these results were reported it was assumed that the observed sulfate and bisulfate bands represented the surface species, based on tests of CO adsorption, comparison of s- and p-polarized spectra, and the obvious potential dependence of the band frequencies [52, 53], the results of the mildly acidic and neutral solutions appear to be inconsistent with those from the other solutions. In the case of the relatively neutral





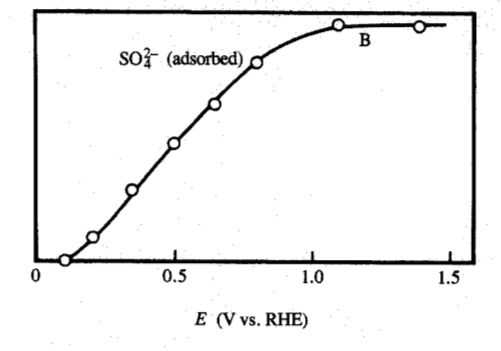


Figure 10

Potential dependence of the intensity of the sulfate ($\simeq 1100~\text{cm}^{-1}$) and bisulfate ($\simeq 1200~\text{cm}^{-1}$) bands for various solutions [52–54]; top: H_2SO_4 solutions; middle: mildly acidic solution containing 0.5 M $\text{Na}_2\text{SO}_4 + 0.01~\text{M}~\text{H}_2\text{SO}_4$; bottom: basic solution containing 0.5 M $\text{Na}_2\text{SO}_4 + 0.0025~\text{M}~\text{NaOH}$. From [54], reproduced with permission.

solutions, the spectra obtained via PDIRS include appreciable contributions from the bulk anions in the thin-layer cell whose concentration changes with potential² [57]. This is an effect pointed out by Bae et al. [58, 59] which is discussed here, since it can affect the interpretation of PDIRS measurements in general.

As mentioned in the second paragraph in the section on adsorption of cyanide, the electrochemical IRRAS detects not only the species on the electrode surface, but also species in the solution near the electrode. This can be seen from the electric field distribution of the light along the electrode surface normal, calculated from the Fresnel equations for stratified media [7]. The field for p-polarized light decreases slowly when the infrared wavelengths are of the order of 10 μ m over the thickness of the cell, which is around 2-3 μ m thick. Thus, if the bulk concentration of the solutes remains unchanged with potential, taking the difference at two different potentials results in the cancellation of the bands due to the bulk species. Generally this is not the case, and if the bands of the bulk species and of the surface species overlap, this can lead to confusion. During the time required to collect a spectrum, the thin-layer cell can be considered to be diffusionally decoupled from the rest of the electrochemical cell, where the counter and reference electrodes are located [60]. However, charge compensation in response to change of the electrode potential takes place rather quickly. The effect on PDIRS of ion migration in and out of the thinlayer cell has been discussed, with examples by Corrigan and Weaver [61]. More recently, Bae et al. [58, 59] have discussed the bulk changes in the thin layer as a function of the electrode potential, especially the change in pH and its influence on the solution composition. For Pt electrodes, protons are supplied to the thin layer from the electrode in two stages as it is made more positive; in the hydrogen region by the desorption of the hydrogen as

$$Pt + H \rightarrow Pt + H^+ + e^-$$

and in the oxygen region by electrode oxidation as

Pt +
$$H_1O \rightarrow PtO + 2H^+ + 2e^-$$
.

The reference potential, 0.05 V (RHE), is in the hydrogen adsorption region for the Pt electrode. As the potential is shifted positively to the sample potential, the desorbed hydrogen brings about a net increase in the hydronium ions in the thin layer² [57]. The effect of hydronium generation at the electrode surface on the thin layer is especially pronounced in the "weakly acid" or "neutral" solutions [54, 55] in which the majority cations are Na⁺ ions, and the majority anions are bisulfate/sulfate ions of relatively lower mobility. A quantitative estimate of these changes can be made if the thickness of the electrolyte,

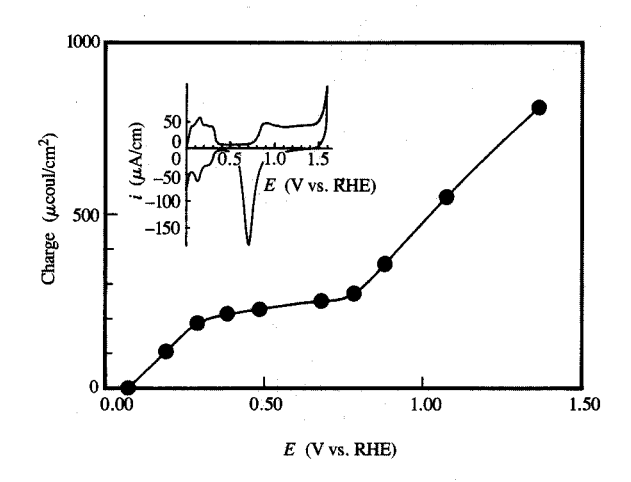


Figure 11

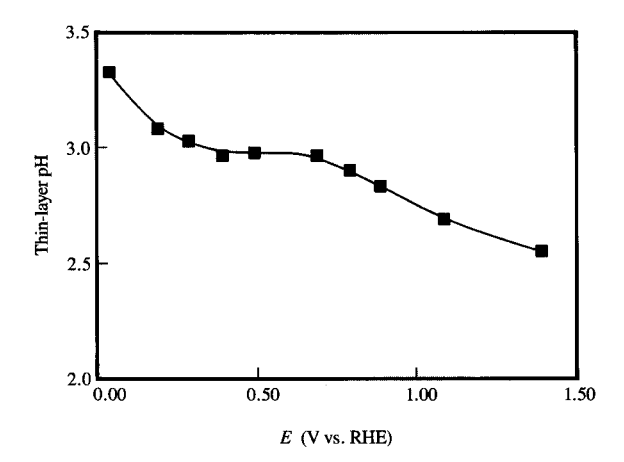
Semiquantitative plot of the accumulated charge density as a function of potential obtained from the cyclic voltammetry of Pt in the solution of 0.5 M Na₂SO₄ and 0.01 M H₂SO₄ corresponding to the cyclic voltammogram in the inset. (I. T. Bae, D. Scherson, K. Kunimatsu, M. G. Samant, and H. Seki, unpublished work.)

the transference numbers of the ions, and the acid-base chemistry involved are known.

Here we show, as an example, the results estimated for the "mildly acid" solution [54], assuming a cell thickness of 1 μ m. The transference numbers of the ions are estimated from the dilute ion mobilities, and the value of the pK of the bisulfate ions based on the dissociation constant is assumed to be 1.99. Furthermore, it is assumed, for simplicity, that the concentration in the layer is uniform. Figure 11 shows a semiquantitative plot of the accumulated charge per square centimeter as a function of potential, obtained by integrating the cyclic voltammogram (see inset). By using the transference numbers estimated from the dilute ion mobilities and the ion concentration of the starting solution at 0.05 V, the thin-layer pH can be obtained as a function of the potential, as shown in Figure 12. On the basis of the mole fraction of the bisulfate and sulfate as a function of pH calculated from the dissociation constant, the concentrations of HSO₄⁻ and SO₄²⁻ in the range of 0.05 and 1.45 V (RHE) are obtained as shown in curve A (HSO₄) and curve B (SO₄²⁻) in Figure 13.

These curves are qualitatively similar to the potential dependence shown in Figure 10 of the band intensity for the "mildly acid" solution (Figure 5 of [54] and Figure 4 of [55]). It is concluded that there is a considerable contribution by the bulk species to the PDIRS for the "mildly acid" and "neutral" solutions. The inadequacy

² I. T. Bae, D. Scherson, K. Kunimatsu, M. G. Samant, and H. Seki, unpublished work.



Solution pH in the thin layer as a function of potential for the system of Figure 9. (I. T. Bae, D. Scherson, K. Kunimatsu, M. G. Samant, and H. Seki, unpublished work.)

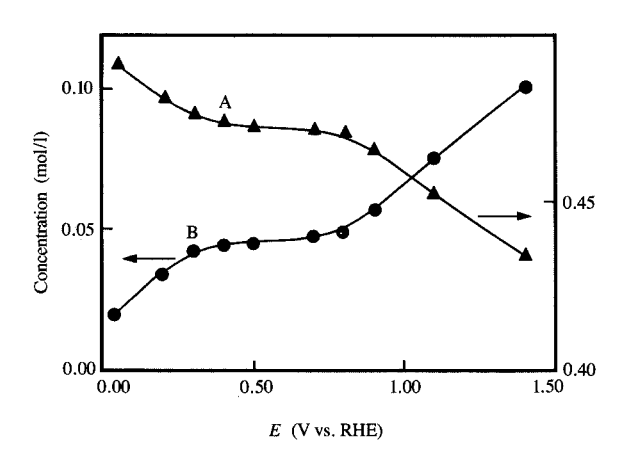


Figure 13

Calculated concentrations of HSO_4^- (curve A) and $SO_4^{2^-}$ (curve B) in the range betwen 0.05 and 1.45 V (RHE) using as a reference the concentration of these species at 0.05 V. The assumptions embodied in the calculations are specified in the text. (I. T. Bae, D. Scherson, K. Kunimatsu, M. G. Samant, and H. Seki, unpublished work.)

of the tests for demonstrating that the bands are due to surface species, the CO adsorption, and the differences due to p- and s-polarization has been fully explained by Iwashita and Nart [57] and is not repeated here. The small but definite frequency shift of the band frequencies indicates that the bands of the adsorbed ions are included in the data.

Single-crystal electrodes

The measurements discussed above were obtained using polycrystalline electrodes, but it should be mentioned that, as demonstrated by the classical work of Clavilier et al. [62], there are subtle differences in the electrochemical behavior between each low-index surface of a platinum single-crystal electrode. Indeed, the investigation of electrodes by ex situ measurements in UHV has long been focused on well-defined single-crystal surfaces, as seen for example in [63]. Recently, procedures have been developed to prepare clean single-crystal surfaces reproducibly in electrolytes [62, 64], together with electrochemical techniques for recognizing the preparation of a clean surface, e.g., the cyclic voltammogram pattern of the hydrogen adsorption-desorption of the Pt electrode [65] and associated confirmation of the clean surface state via UHV surface analysis techniques [66]. Consequently, in situ IRRAS measurements on single-crystal electrode surfaces have appeared [67-70] which indicate that the IR bands observed are indeed generally quite distinct for each low-index surface.

Recently there has been a prolific output from Weaver and his group [71–87] involving IRRAS of single-crystal electrodes. Here we focus on one of the most significant results to have evolved from these investigations; i.e., a very plausible link between the IRRAS measurements in UHV and in an electrolyte [85] has been established. This link is provided with the aid of the following relationship discussed by Trasatti [88] for the difference between the electrochemical potential (relative to a reference electrode) E^M and the corresponding electron work function ϕ^M if the electrode were in UHV:

$$E^M - \phi^M/e = \nabla \chi^M - g^s(\text{dip}) + g_s^M(\text{ion}) + \chi_s - E_K(\text{ref}),$$

where $\nabla \chi^M$ reflects the change in the work function due to the metal contacting the solution, $g^s(\text{dip})$ and $g^M_s(\text{ion})$ are the contributions of the solvent dipoles and the ionic charges to the metal-solution potential drop, χ_s is the surface potential of the solution-vacuum interface, and $E_K(\text{ref})$ is the "absolute" potential of the reference electrode. Although the values of the above parameters are not known exactly, they have been estimated on the basis of experimental and theoretical considerations [85]. Accordingly, the results of the field-dependent peak frequency of the CO stretching mode on the Pt and Rh electrodes [74–83] have been plotted in combination with the measured frequency and the work function of the same electrode with CO adsorbed in UHV (see for example references in [79]). This result [85] is reproduced here as

Figure 14, in which the field-dependent CO frequency data (solid lines) taken in the electrochemical cell are extrapolated to the points (in open symbols) which are close to data points (filled symbols) obtained in UHV. The extrapolation was necessary because there is a limit to the electrode potential in an aqueous solution due to oxidation. This limitation has been overcome more recently by carrying out measurements in nonaqueous solutions [86, 87] in which the ideally polarizable region extends to higher potentials. The measurements provided points on the extrapolated line, further substantiating the above relationship and the values of the parameters used therein.

Concluding remarks

Examples of investigations, primarily in our laboratory, involving the use of in situ vibrational spectroscopy of the electrolyte interface, have been reviewed. The examples demonstrate the kind of insight such investigations can provide. The ability to control the potential and hence the field applied to the adsorbate provides a powerful means of investigating adsorbate-substrate interactions in an electrochemical system. The potential-dependent shift of the vibrational band can serve to identify whether the source is a surface species. The studies using CO and CN illustrate that insight into the mechanisms underlying this shift can be gained in molecular detail through ab initio calculations involving SCF wavefunctions of clusters. The contrasting difference of the dominantly covalent nature of the metal-to-CO bond and the dominantly ionic nature of the metal-to-CN bond could not have been understood from only spectroscopic data.

The difficulty encountered in the interpretation of the IRRAS of the Pt electrode bisulfate and sulfate solutions illustrates one of the fundamental problems of IRRAS, i.e., the identification of bands associated with surface species. As the spectral region is extended to longer wavelengths, this problem becomes increasingly severe. With all its uncertainty, an important advantage of SERS is that it is highly surface-specific; it played a significant complementary role to IRRAS in the investigation of CN adsorption. Recently a very promising, highly surfacespecific technique called "sum frequency generation" (SFG) [89] has been developed by Shen and his students. Its surface specificity is derived from the fact that it is a nonlinear optical process related to the better-known second harmonic generation (SHG) phenomenon. It derives its surface specificity from the principle that a second-order nonlinear process is forbidden in a medium with inversion symmetry and the fact that such symmetry is broken at an interface.

Guyot-Sionnest and Tadjeddine have provided the first demonstration of the SFG technique on an electrode-electrolyte system [90], clearly indicating submonolayer sensitivity. From phase considerations, the

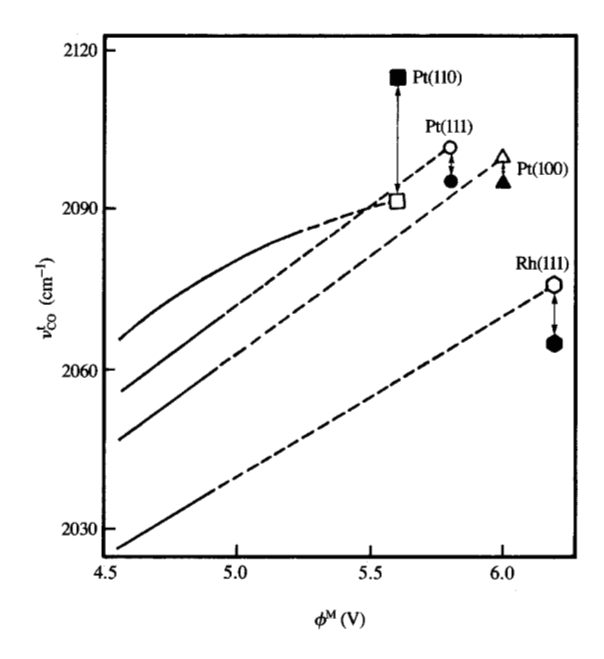


Figure 14

Comparison of the $\nu_{\rm CO}$ frequency-electrode potential (solid line) for terminally coordinated CO at saturation coverage with associated metal UHV data, shown as filled symbols. The electrochemical potential (vs. NHE) has been converted to the equivalent vacuum work function $\phi^{\rm M}$ by the equation given in the text. From [85], reproduced with permission.

results indicated that on a Pt electrode the CN ion is adsorbed in two different orientations, one with the carbon atom adjacent to the metal and the other with the nitrogen atom adjacent to the metal. Previous IRRAS measurement of the Pt electrode [35] did not reveal this, and UHV ex situ measurements on a Pt(111) surface [64] did not suggest this possibility. There is probably still room for debate regarding the interpretation of the SFG data, but the results obtained are provocative and suggest that the technique is likely to become very effective in the investigation of the electrode–electrolyte interface. Since the technique involves the use of subnanosecond laser pulses, it may make it possible to monitor transient phenomena at the electrode.

The measurements on well-defined single-crystal electrodes have added the refinement necessary to link the measurements in electrochemical cells to those in UHV. This was done for Pt and Rh electrodes having a saturation coverage of CO. Having established this link, we should be in a better position to extract information regarding the interaction of the adsorbed species with the solvent and

electrolyte molecules from IRRAS measurements. Because of the rapid advances in computer technology, we should see increasingly sophisticated analyses of more complex molecules and clusters, of interactions between adsorbate and solvent molecules, and of effects due to the use of different electrode metals. We can also expect to see collaborative work in combination with other *in situ* techniques such as those involving the use of differential capacitance measurements, radiotracer measurements, quartz crystal microbalance measurements, and X-ray scattering and diffraction.

Acknowledgments

The IBM-related work described here was supported in part by the Office of Naval Research. A large part of it was carried out in collaboration with my colleagues, K. Ashley, P. S. Bagus, W. G. Golden, J. G. Gordon, K. Kunimatsu, C. J. Nelin, M. R. Philpott, and M. G. Samant. I have benefitted greatly from this pleasant interaction, for which I am very grateful. I also wish to thank M. J. Weaver for permission to use Figure 1 from [8]. Finally, I thank O. Melroy for his support and constructive comments regarding the manuscript.

References

- 1. D. J. Jeanmaire and R. P. Van Duyne, J. Electroanal. Chem. 84, 1 (1977).
- 2. J. A. Creighton, J. Amer. Chem. Soc. 99, 5215 (1977).
- (a) A. Bewick, K. Kunimatsu, and S. B. Pons, Electrochim. Acta 25, 465 (1980). (b) A. Bewick and K. Kunimatsu, Surf. Sci. 101, 131 (1980).
- Surface Enhanced Raman Scattering, R. K. Chang and T. K. Furtak, Eds., Plenum Press, New York, 1982.
- 5. R. G. Greenler, J. Chem. Phys. 44, 310 (1966).
- 6. F. M. Hoffman, Surf. Sci. Rep. 3, 107 (1983) and references therein.
- H. Seki, K. Kunimatsu, and W. G. Golden, *Appl. Spectrosc.* 39, 437 (1984).
- 8. H. Seki, in *Electrochemical Surface Science*, ACS Symposium Series **378**, M. P. Soriaga, Ed., 1988.
- 9. B. Beden, C. Lamy, A. Bewick, and K. Kunimatsu, J. Electroanal. Chem. 122, 343 (1981).
- 10. A. Bewick and S. Pons, Adv. Infrared Raman Spectrosc. 12, 1 (1985).
- D. S. Corrigan and M. J. Weaver, J. Phys. Chem. 90, 5300 (1986).
- D. S. Corrigan, L. H. Leung, and M. J. Weaver, *Anal. Chem.* 59, 2252 (1987).
- 13. W. G. Golden, D. S. Dunn, and J. Overend, *J. Catal.* 71, 395 (1981).
- 14. W. G. Golden and D. D. Saperstein, J. Electron. Spectrosc. 30, 43 (1983).
- 15. P. R. Mahaffy and M. J. Dignam, Surf. Sci. 97, 377 (1980).
- 16. A. Otto, Surf. Sci. 75, L392 (1978).
- 17. T. E. Furtak, Solid State Commun. 28, 903 (1978).
- 18. M. Fleischmann, I. R. Hill, and M. E. Pemble, *J. Electroanal. Chem.* **136**, 362 (1982).
- H. Baltruschat and M. Vielstich, J. Electroanal. Chem. 154, 141 (1983).
- H. Baltruschat and J. Heitbaum, J. Electroanal. Chem. 157, 319 (1983).
- H. Seki, K. Kunimatsu, and W. G. Golden, presented at the meeting of the International Society of Electrochemistry, Berkeley, CA, 1984.

- K. Kunimatsu, H. Seki, and W. G. Golden, *Chem. Phys. Lett.* 108, 195 (1984).
- K. Kunimatsu, H. Seki, W. G. Golden, J. G. Gordon II, and M. R. Philpott, Surf. Sci. 158, 596 (1985).
- L. H. Jones and R. A. Penneman, J. Chem. Phys. 22, 965 (1954).
- K. Kunimatsu, H. Seki, W. G. Golden, J. G. Gordon II, and M. R. Philpott, *Langmuir* 4, 337 (1988).
- R. Kötz and E. Yeager, J. Electroanal. Chem. 123, 335 (1981).
- 27. W. Wetzel, H. Gerischer, and B. Pettinger, *Chem. Phys. Lett.* **80**, 159 (1981).
- 28. K. Kunimatsu, J. Electroanal. Chem. 140, 205 (1982).
- J. W. Russell, J. Overend, K. Scanlon, M. Severson, and A. Bewick, J. Phys. Chem. 86, 3066 (1982).
- 30. D. K. Lambert, Solid State Commun. 51, 297 (1984).
- 31. K. Kunimatsu, W. G. Golden, H. Seki, and M. R. Philpott, *Langmuir* 1, 245 (1985).
- 32. K. Kunimatsu, H. Seki, W. G. Golden, J. G. Gordon II, and M. R. Philpott, *Langmuir* 2, 464 (1986).
- K. A. B. Lee, K. Kunimatsu, J. G. Gordon II, W. G. Golden, and H. Seki, *J. Electrochem. Soc.* 134, 1676 (1987).
- 34. R. A. Shigeishi and D. A. King, Surf. Sci. 58, 379 (1976).
- K. Ashley, M. Lazaga, M. G. Samant, H. Seki, and M. R. Philpott, Surf. Sci. Lett. 219, L590 (1989).
- K. Ashley, F. Weinert, M. G. Samant, H. Seki, and M. R. Philpott, J. Phys. Chem. 95, 7409 (1991).
- D. A. King, in Vibrational Spectroscopy of Adsorbates,
 R. F. Willis, Ed., Springer Series in Chemical Physics,
 Vol. 15, Springer-Verlag, Berlin, 1980.
- 38. B. E. Hayden, and A. M. Bradshaw, Surf. Sci. 125, 787 (1983).
- 39. F. A. Cotton and G. Wilkinson, *Advanced Inorganic Chemistry*, 3rd ed., John Wiley, Inc., New York, 1972.
- 40. G. Blyholder, J. Phys. Chem. 68, 2778 (1964).
- 41. N. K. Ray and A. B. Anderson, *J. Phys. Chem.* **86**, 4851 (1982)
- 42. S. Holloway and J. K. Norskov, *J. Electroanal. Chem.* **161**, 193 (1984).
- A. B. Anderson, R. Kötz, and E. Yeager, Chem. Phys. Lett. 82, 130 (1981).
- (a) D. K. Lambert, J. Electron. Spectrosc. 30, 59 (1983);
 (b) D. K. Lambert, Phys. Rev. Lett. 50, 2106 (1983);
 (c) D. K. Lambert, Solid State Commun. 51, 297 (1984).
- P. S. Bagus, K. Hermann, and M. Seel, J. Vac. Sci. Technol. 18, 435 (1981).
- (a) P. S. Bagus, C. J. Nelin, and C. W. Bauschlicher, *Phys. Rev. B* 28, 5423 (1983); (b) P. S. Bagus, C. J. Nelin, and C. W. Bauschlicher, *J. Vac. Sci. Technol. A* 2, 905 (1984).
- (a) P. S. Bagus and W. Müller, Chem. Phys. Lett. 115, 540 (1985);
 (b) W. Müller and P. S. Bagus, J. Vac. Sci. Technol. A 3, 1623 (1985);
 (c) W. Müller and P. S. Bagus, J. Electron. Spectrosc. 38, 103 (1986).
- P. S. Bagus, C. J. Nelin, W. Müller, M. R. Philpott, and H. Seki, *Phys. Rev. Lett.* 58, 559 (1987).
- P. S. Bagus, C. J. Nelin, K. Hermann, and M. R. Philpott, *Phys. Rev. B* 36, 8169 (1987).
- (a) H. F. Schaefer III, Electronic Structure of Atoms and Molecules, Addison-Wesley Publishing Co., Reading, MA, 1972;
 (b) H. F. Schaefer III, Quantum Chemistry, Clarendon Press, Oxford, U.K., 1984.
- 51. C. W. Bauschlicher, Chem. Phys. Lett. 118, 307 (1985).
- 52. K. Kunimatsu, M. G. Samant, H. Seki, and M. R. Philpott, *J. Electroanal. Chem.* 243, 203 (1988).
- K. Kunimatsu, M. G. Samant, and H. Seki, J. Electroanal. Chem. 258, 163 (1989).
- 54. K. Kunimatsu, M. G. Samant, and H. Seki, *J. Electroanal. Chem.* **272**, 185 (1989).

- M. G. Samant, K. Kunimatsu, H. Seki, and M. R. Philpott, J. Electroanal. Chem. 391, 391 (1990).
- G. Horanyi, J. Solt, and F. Nagy, J. Electroanal. Chem. 31, 95 (1971).
- T. Iwashita and F. C. Nart, J. Electroanal. Chem. 295, 215 (1990).
- I. T. Bae, X. Xing, D. Scherson, and E. B. Yeager, *Anal. Chem.* 61, 1164 (1989).
- I. F. T. Bae, D. Scherson, and E. B. Yeager, *Anal. Chem.* 62, 45 (1990).
- A. T. Hubbard and F. C. Anson, in *Electroanalytical Chemistry*, Vol. 4, A. J. Bard, Ed., Marcel Dekker, New York, 1971, p. 129.
- D. S. Corrigan and M. J. Weaver, J. Electroanal. Chem. 239, 55 (1988).
- (a) J. Clavilier, R. Faure, G. Guinet, and R. Durand, J. Electroanal. Chem. 107, 205 (1980); (b) J. Clavilier, J. Electroanal. Chem. 107, 211 (1980).
- S. D. Rosasco, J. L. Stickney, G. N. Salaita, D. G. Frank, J. Y. Katekaru, B. C. Schardt, M. P. Soriaga, D. A. Stern, and A. T. Hubbard, *J. Electroanal. Chem.* 188, 95 (1985).
- 64. (a) M. Hourani and A. Wieckowski, J. Electroanal. Chem. 227, 259 (1987); (b) D. Zurawski, L. Rice, M. Hourani, and A. Wieckowski, J. Electroanal. Chem. 230, 221 (1987).
- J. Clavilier and D. Armand, J. Electroanal. Chem. 199, 187 (1986).
- F. T. Wagner and P. N. Ross, Jr., J. Electroanal. Chem. 250, 301 (1988).
- (a) S. Juanto, B. Beden, F. Hahn, J. M. Leger, and C. Lamy, J. Electroanal. Chem. 237, 119 (1987); (b) B. Beden, S. Juanto, J. M. Leger, and C. Lamy, J. Electroanal. Chem. 238, 323 (1987).
- (a) F. Kitamura, M. Takeda, M. Takahashi, and M. Ito, *Chem. Phys. Lett.* 142, 318 (1987); (b) F. Kitamura, M. Takahashi, and M. Ito, *J. Phys. Chem.* 72, 3230 (1988).
- N. Furuya, S. Motoo, and K. Kunimatsu, J. Electroanal. Chem. 239, 347 (1988).
- S. G. Sun, J. Clavilier, and A. Bewick, J. Electroanal. Chem. 240, 147 (1988).
- L.-W. H. Leung, S.-C. Chang, and M. J. Weaver, *Chem. Phys. Lett.* 90, 7426 (1989).
- S.-C. Chang, L.-W. H. Leung, and M. J. Weaver, J. Phys. Chem. 93, 5341 (1989).
- L.-W. H. Leung and M. J. Weaver, J. Phys. Chem. 93, 7218 (1989).
- L.-W. H. Leung, S.-C. Chang, and M. J. Weaver, J. Electroanal. Chem. 266, 317 (1989).
- 75. S.-C. Chang and M. J. Weaver, J. Chem. Phys. 92, 4582 (1990).
- S.-C. Chang and M. J. Weaver, J. Phys. Chem. 94, 5095 (1990).
- S.-C. Chang, L.-W. H. Leung, and M. J. Weaver, J. Phys. Chem. 94, 6013 (1990).
- 78. S.-C. Chang and M. J. Weaver, Surf. Sci. 230, 222 (1990).
- 79. S.-C. Chang and M. J. Weaver, Surf. Sci. 238, 142 (1990). 80. S.-C. Chang and M. J. Weaver, J. Electroanal. Chem.
- S.-C. Chang and M. J. Weaver, J. Electroanal. Chem 285, 263 (1990).
- 81. J. D. Roth, S.-C. Chang, and M. J. Weaver, J. Electroanal. Chem. 288, 255 (1990).
- 82. S.-C. Chang and M. J. Weaver, Surf. Sci. 241, 11 (1991).
- 83. S.-C. Chang, J. D. Roth, and M. J. Weaver, *Surf. Sci.* **244**, 113 (1991).
- S.-C. Chang, A. Hamelin, and M. J. Weaver, Surf. Sci. 239, L543 (1990).
- S.-C. Chang and M. J. Weaver, J. Phys. Chem. 95, 5391 (1991).
- S.-C. Chang, A. Hamelin, and M. J. Weaver, J. Phys. Chem. 95, 5560 (1991).
- 87. X. Jiang and M. J. Weaver, Surf. Sci. 275, 235 (1992).

- 88. Sergio Trasatti, J. Electroanal. Chem. 150, 1 (1983).
- 89. Y. R. Shen, Nature 337, 519 (1989).
- 90. P. Guyot-Sionnest and A. Tadjeddine, Chem. Phys. Lett. 172, 341 (1990).

Received January 21, 1992; accepted for publication March 4, 1993

Hajime Seki IBM Research Division, Almaden Research Center, 650 Harry Road, San Jose, California 95120 (HAJSEKI at ALMADEN, hajseki@almaden.ibm.com). Dr. Seki is a Research Staff Member in the Physical Sciences Department at the Almaden Research Center. He received his B.S. degree in physics from Brown University in 1954, and his M.S. and Ph.D. degrees in physics from the University of Pennsylvania in 1956 and 1961, respectively; his Ph.D. thesis was on liquid helium. Dr. Seki began his IBM career at the Thomas J. Watson Research Center in its superconducting cryotron program, transferring to the Almaden Research Center in 1966 to work on low-mobility photoconductors and electrophotography. Since then he has worked in the areas of electrochemical displays, molecular crystals, surface-enhanced Raman scattering, CVD diamond, tribology, and storage technology. Recently he joined the Center for Computational Chemistry in Almaden. Dr. Seki is a member of the American Physical Society, the American Chemical Society, the American Association for the Advancement of Science, and the Japanese Physical Society.

